Bioorg. Med. Chem. Lett. 60 (2022) 128588

Contents lists available at ScienceDirect

Bioorganic & Medicinal Chemistry Letters

journal homepage: www.elsevier.com/locate/bmcl

Development of dihydropyrrolopyridinone-based PKN2/PRK2 chemical tools to enable drug discovery

Fiona Scott [a,1], Angela M. Fala [b,c,1], Jessica E. Takarada [b,c], Mihaela P. Ficu [a], Lewis E. Pennicott [a], Tristan D. Reuillon [a], Rafael M. Couñago [b,c], Katlin B. Massirer [b,c,*], Jonathan M. Elkins [c,d,*], Simon E. Ward [e,*]

[a] Sussex Drug Discovery Centre, University of Sussex, Sussex House, Falmer, Brighton BN1 9RH, United Kingdom
[b] Centro de Química Medicinal (CQMED), Centro de Biologia Molecular e Engenharia Genética (CBMEG), Universidade Estadual de Campinas (UNICAMP), Campinas, SP 13083-875, Brazil
[c] Structural Genomics Consortium, Departamento de Genética e Evolução, Instituto de Biologia, UNICAMP, Campinas, SP 13083-886, Brazil
[d] Structural Genomics Consortium, Nuffield Department of Medicine, University of Oxford, Oxford OX3 7DQ, United Kingdom
[e] Medicines Discovery Institute, Cardiff University, Main Building, Park Place, Cardiff CF10 3AT, United Kingdom

ARTICLE INFO

Keywords:
PKN2
PRK2
PKN1
Dihydropyrrolopyridinone
Kinase inhibitors
Chemical tools

ABSTRACT

The Protein Kinase N proteins (PKN1, PKN2 and PKN3) are Rho GTPase effectors. They are involved in several biological processes such as cytoskeleton organization, cell mobility, adhesion, and cell cycle. Recently PKNs have been reported as essential for survival in several tumor cell lines, including prostate and breast cancer. Here, we report the development of dihydropyrrolopyridinone-based inhibitors for PKN2 and its closest homologue, PKN1, and their associated structure–activity relationship (SAR). Our studies identified a range of molecules with high potency exemplified by compound 8 with $K_i = 8$ nM for PKN2 and 14x selectivity over PKN1. Membrane permeability and target engagement for PKN2 were assessed by a NanoBRET cellular assay. Importantly, good selectivity across the wider human kinome and other kinase family members was achieved. These compounds provide strong starting points for lead optimization to PKN1/2 development compounds.

The Protein Kinase N (protein kinase novel, PKN, also known as protein kinase C-related kinases, PRKs) proteins belong to the AGC group of serine/threonine kinases (named after protein kinase A, G, and C families - PKA, PKC, PKG).[1,2] PKN proteins have a conserved domain architecture in which three *N*-terminal antiparallel coiled-coil domains (ACC1-3) are followed by a central, lipid-binding, regulatory domain (C2-like) and a C-terminal catalytic serine/threonine kinase domain (K_D). In mammals, the PKN sub-family consists of three members - PKN1, PKN2, and PKN3.[1,2] PKN2 and PKN3 have additional proline-rich regions between their C2-like and kinase domains. All three PKN proteins share high sequence similarity but differ in their regulatory mechanisms and tissue distributions. PKN3 expression is restricted to certain tissues, such as skeletal muscle, heart, and liver, whereas PKN1 and PKN2 are ubiquitously expressed.[3–7]

PKN proteins differ in their ability to interact with members of the Rho family of small GTPases *via* their ACC domains and with phospholipids, fatty acids, and arachidonic acid *via* their C2-like domains. Full activation of PKN proteins require phosphorylation of their activation loops by phosphoinositide-dependent kinase 1 (PKD1), which is in turn dependent on PKN-Rho GTPase interaction.[1] Rho-family GTPases play critical roles during cytoskeleton re-organization and cell migration.[8] Likewise, PKN proteins are thought to participate in a variety of cellular

Abbreviations: ACC1-3, antiparallel coiled-coil domains; ATP, adenosine triphosphate; ATPγS, ATP-gamma-sulfate; BRET, bioluminescence resonance energy transfer; C2-like, central, lipid-binding, regulatory domain; ChEMBL, European Molecular Biology Laboratory Chemical database; FDA, United States Food and Drug Administration; GTPase, guanosine-5′-triphosphatase; HEK, human embryonic kidney cells; IC_{50}, half-maximal inhibitory constant; K_D, kinase domain; K_i, inhibitory constant; MAPK, mitogen-activated protein kinase; MAPKAPK2, MAPK-activated protein kinase 2; NB, no binding; PDB, protein database; PKA, protein kinase A; PKC, protein kinase C; PKD1, phosphoinositide-dependent kinase 1; PKG, protein kinase G; PKN, protein kinase N; RNAi, ribonucleic acid interference; ROCK, Rho-associated, coiled-coil-containing protien kinase; SAR, structure-activity relationship; TR-FRET, time-resolved fluorescence.

* Corresponding authors at: Medicines Discovery Institute, Cardiff University, Cardiff, CF10 3AT, United Kingdom.
E-mail addresses: kmassire@unicamp.br (K.B. Massirer), jon.elkins@cmd.ox.ac.uk (J.M. Elkins), wards10@cardiff.ac.uk (S.E. Ward).

[1] These authors contributed equally.

https://doi.org/10.1016/j.bmcl.2022.128588
Received 11 December 2021; Received in revised form 14 January 2022; Accepted 22 January 2022
Available online 29 January 2022

processes that require cytoskeleton remodeling, including cell cycle regulation, receptor trafficking, vesicle transport, and apoptosis.[9–11]

Modulation of PKN kinase activity has been suggested as a possible therapeutic strategy for a variety of conditions. PKN1 has been mostly associated with neurodegenerative disorders and, in combination with PKN2, has been implicated in tumor cell invasion of bladder tumor.[12] PKN2 has been shown essential for survival in various cancer cell lines, including prostate, and breast cancer.[13–15] RNAi-mediated knockdown of PKN3 in mouse models showed a decrease in the growth of prostate and pancreatic tumors, and prevented lung metastases.[16,17] The Structural Genomics Consortium defines chemical probes as small, drug-like molecules which have in vitro IC_{50} or $K_d < 100$ nM, >30-fold selectivity over proteins in the same family, significant on-target cellular activity at 1 μM and an appropriate negative control compound.[18] By this definition, there are not currently any suitably potent and selective inhibitors available for studying the cellular functions or therapeutic potential of the PKN proteins.

To identify promising starting points for PKN2-selective inhibitors, we performed a search of the chemical database ChEMBL for existing compounds with biological activity against this enzyme.[19] This search returned ~1200 compounds that were ranked by potency. Our previous work[20] describes an attempt to optimize the most potent of these compounds.

Compound **3** was also selected for its nanomolar potency against PKN2 ($K_i = 5$ nM). The compound was originally developed as part of a program developing a MAPKAPK2 inhibitor.[21] Compound **3** has a high ligand efficiency, and an interesting core, not yet seen in any FDA approved kinase inhibitor,[22] which provides multiple vectors that could be explored in a medicinal chemistry project. Here, we report the synthesis and structure–activity relationship (SAR) studies of **3** for a repurposed application as a PKN2 inhibitor.

Compound **3** was successfully synthesized *via* a condensation reaction between commercially available 4-(bromoacetyl) pyridine hydrobromide (**1**) piperidin-2,4-dione (**2**) and ammonium acetate[21] (Fig. 1).

A set of derivatives of **3** were prepared, aiming to identify favorable substitutions for PKN2 interaction according to the synthetic route from Scheme 1 with yields ranging between 3% and 87%. 3-Pyridyl (**4**), 2-pyridyl (**5**) and phenyl (**6**) analogues were synthesized by using their corresponding bromoacetyl reagents. Compounds **7**–**12** were similarly prepared by substituting ammonium acetate with the necessary alkyl amine, e.g., methyl amine to produce compound **7**. Further alkylation of the lactam N—H was achieved by treating *N*-ethyl- substituted compound **8** with sodium hydride followed by the addition of methyl iodide or *n*-propyl iodide to generate compounds **13** and **14**, respectively.[23] Analogues **15–17** were obtained by substituting piperidine-2,4-dione with commercial reagents *tert*-butyl 4-oxo-piperidine-1-carboxylate, 1,3-cyclohexanedione, and 6-phenylpiperidine-2,4-dione, respectively.

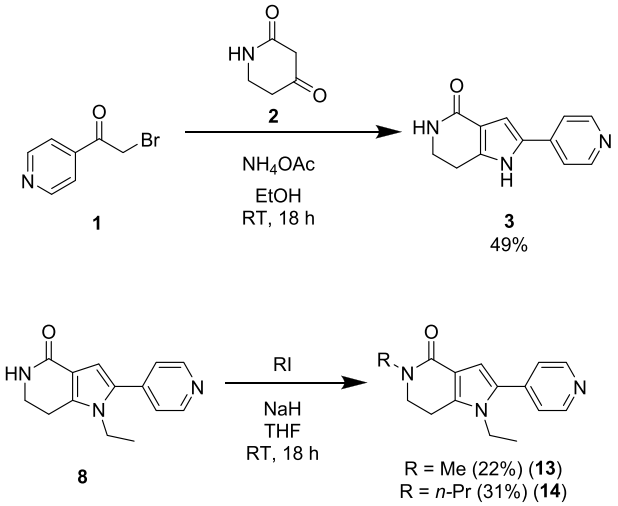

Fig. 1. Synthesis of compounds **3**, **13** and **14.**

To obtain the likely binding mode and to guide our synthetic efforts, we docked **3** into the ATP-binding site of the available PKN2 structure bound to ATPγS (PDB ID 4CRS) using the Schrodinger software suite (Fig. 2). The analysis suggests that **3** is anchored to PKN2′s hinge region *via* a hydrogen bond facilitated by the 4-pyridine nitrogen in the main chain of an alanine residue (A740) and with side chain of the catalytic lysine (K686). This predicted binding mode matches that observed for a 2-(2-fluorophenyl)-pyridine analog of **3** in a co-crystal structure with MAPKAPK2 (PDB ID 2P3G).[21]

The kinase domains of PKN1 and PKN2 share ~80% sequence identity and, considering residues within 5 Å of bound ATP, there are only two amino acid differences between the ATP-binding sites of these two proteins. The structural equivalent of L664 in the P-loop of PKN2 is G628 in PKN1, and A740 in the hinge region of PKN2 is S704 in PKN1.

To measure the binding affinities (K_i) of the synthesized compounds for PKN2, we employed a TR-FRET-based, tracer displacement assay. IC_{50} values were determined, and K_i values were calculated from these IC_{50} values using the Cheng-Prusoff equation to allow comparison of binding of the inhibitors to PKN1 or PKN2, independent of the affinity of the tracer for each kinase.[24] As we sought to develop PKN2-selective compounds, we wished to calculate the selectivity of each compound for PKN2 over its closest homologue, PKN1. Results from our tracer-displacement assay confirmed compound **3** as a high-affinity ligand of PKN2 ($K_i = 8.0$ nM). Encouragingly, **3** was around 20-fold less potent towards PKN1 ($K_i = 150$ nM) (Table 1).

Replacing the 4-pyridyl group with a 3-pyridyl (**4**), 2-pyridyl (**5**) or phenyl (**6**) ring significantly reduced affinity for PKN2, in line with a previous series developed in-house around a benzimidazole core.[20] These results indicated that the 4-pyridyl group in **3** is indeed important for interaction with the A740 backbone of the PKN2 hinge region, as suggested by our docking studies, and in line with our previous observations with a structurally similar benzimidazole series.[20]

We next explored adding different alkyl groups of varying lengths and composition to the pyrrole N—H in **3**. Our binding results indicated that substituting with a methyl group (**7**) reduced PKN2 and PKN1 potency. Ethyl (**8**) and *n*-propyl (**9**) groups appended to the pyrrole ring, on the other hand, were well-tolerated by PKN2 and PKN1, making them

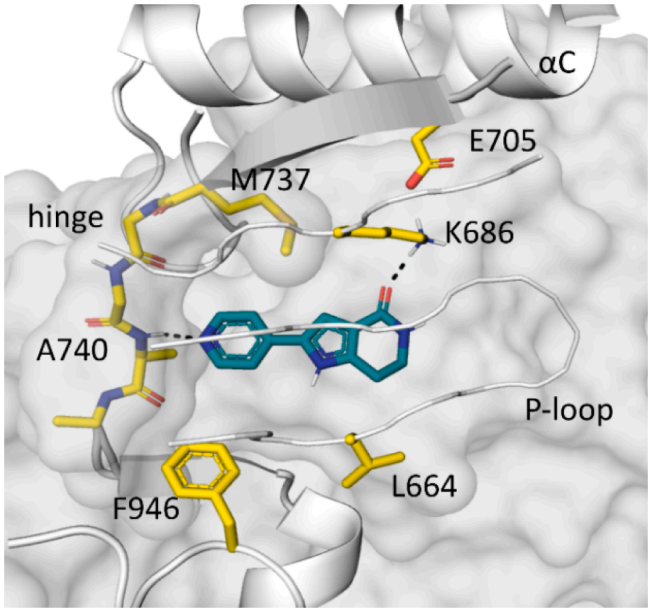

Fig. 2. Molecular docking of PKN2 bound to compound **3**. The 4-pyridyl nitrogen and the lactam carbonyl act as a hydrogen bond acceptor to the main chain amide nitrogen of A740 and the primary amine of K686 respectively.

Table 1
Structure activity relationships for pyrrole compounds binding to PKN2 and PKN1.*

#		PKN2			PKN1			Selectivity (PKN1/PKN2)
		K_i (nM)	**IC_{50} (nM)**	**Standard Deviation (nM)**	**K_i (nM)**	**IC_{50} (nM)**	**Standard Deviation (nM)**	
3**	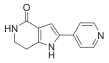	8	16	0.4	150	300	120	18.8
4	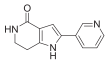	1600	3200	260	–	>5000	–	–
5	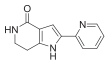	–	NB	–	–	NB	–	–
6	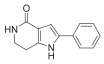	–	NB	–	–	NB	–	–
7	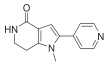	130	260	8	2200	4500	760	16.9
8**	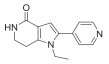	8	16	2	108	210	40	13.5
9**	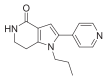	7	15	1	60	120	15	8.6
10	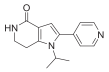	70	140	1	920	1840	200	13.1
11	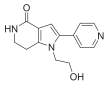	15	30	0.5	220	440	20	14.7
12	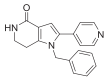	320	640	75	1500	3000	1100	4.7
13	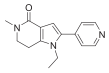	170	350	70	–	>5000	–	–
14	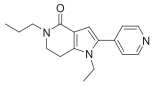	1300	2600	630	–	>5000	–	–
15	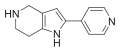	1100	2200	64	–	>5000	–	–
16	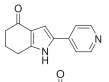	30	60	10	650	1300	400	21.7
17	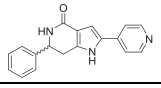	25	50	6	260	520	65	10.4

*Tracer displacement assay measured IC_{50} values and corresponding calculated K_i values for PKN2 and PKN1 are shown in nM. The assay Z' factor was $0.7 > Z' < 0.8$. IC_{50} values for PKN1 and PKN2 are represented as the mean and standard deviation of mean in two independent experiments performed in triplicate. NB = no binding.
** A representative curve of a single technical replicate experiment is shown in Supplementary Fig. S1.

equipotent to **3** for PKN2, with slightly less selectivity over PKN1 compared to **3**. These findings indicated that groups with hydrogen-bonding capacity at this position might not be essential for binding to both PKN proteins, as expected from the likely orientation of the inhibitors in the ATP binding site such that the pyrrole N—H is directed towards the entrance to the binding site. On the other hand, appending bulkier substituents, such as isopropyl (**10**) or benzyl (**12**), had a larger (≥9-fold) negative impact on PKN2 binding, indicating that bulkier substituents at this position are not tolerated. These results were also in agreement with our *in silico* docking analysis.

We then evaluated the impact of changes to the lactam ring of compounds **8** and **3**. Appending a methyl (**13**) or *n*-propyl (**14**) group to the lactam nitrogen atom in **8**, reduced compound binding to PKN2 by ~20- and ~160-fold, respectively. On the other hand, adding a phenyl group adjacent to the lactam in **3**, had a smaller impact (~3-fold) on the binding affinity of compound **17** to PKN2. Finally, we explored the relevance of the lactam nitrogen and carbonyl groups of **3** for binding to PKN2. Removal of the oxygen atom from the lactam ring (**15**) resulted in a severe loss of potency (~150-fold), whereas the replacement of the amide nitrogen with a carbon atom was better tolerated (~4-fold drop in potency). As above, these changes had a similar impact on binding to PKN1 (Table 1).

As previously discussed, PKN1 and PKN2 have very similar ATP-binding pockets. Thus, it was not entirely surprising that all derivatives of compound **3** had some potency for PKN1. To evaluate compound selectivity within the broader human kinome, we tested the ability of **3** and **8** to bind to a panel of 468 human kinases *via* the commercially available DiscoverX KINOME*scan*® panel (Fig. 3 and full datasets in Supplementary Table S1).[25,26] In this assay, compounds were used at 1 μM final concentration and compete for the ATP-binding site of the kinases attached to an immobilized ligand.

From this selectivity experiment, we observed relatively few off-target kinases, with the two compounds affecting less than 5% of the kinase panel. Compound **3** appeared to be potent for ROCK1 and ROCK2 kinases (>70% inhibition); these are kinases that are also from the AGC family. Interestingly, compound **3** only showed 44% inhibition of MAPKAPK2 in this experiment at 1 μM concentration; it was previously reported to have a modest MAPKAPK2 affinity ($IC_{50} = 171$ nM)[21] and so with the difference in assay formats this is perhaps not surprising. Compound **8** showed a similar level of selectivity overall but was less

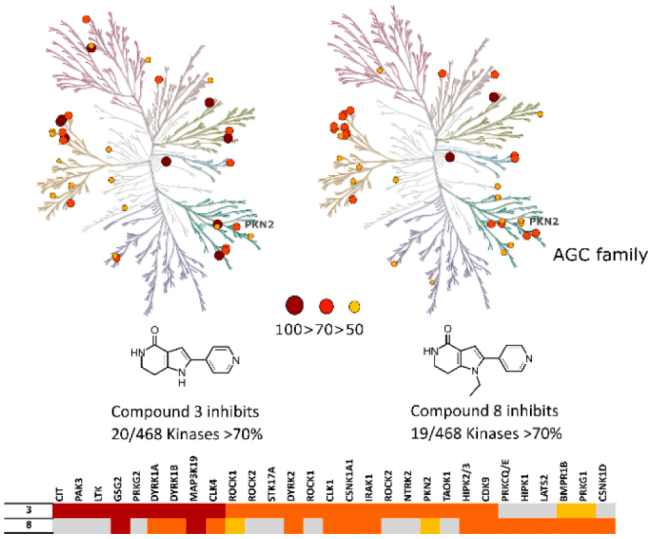

Fig. 3. Phylogenetic kinome tree with relative binding to different protein kinases of compounds **3** and **8,** depicted as colored circles. Larger circle size indicates greater potency. Bottom right dark green branch denotes AGC kinases including PKN2. Colors represent % inhibition, red ≥90%, orange ≥70% and yellow ≥50%. Figure made with KinMap (http://www.kinhub.org/kinmap/).

potent (<50% of inhibition) towards both ROCK kinases. This suggests that this selectivity screen has a maximum power limit of 10-fold selectivity relative to PKN2.

To test the ability of **3**, **8**, **9** and **11** to bind to PKN2 in cells we used a cell-based target engagement assay (NanoBRET, Promega).[27] In this assay, the kinase is fused to luciferase (NanoLuc) and is ectopically expressed in human (HEK293) cells. The cells are incubated with a fluorescent version of a promiscuous kinase inhibitor, referred to as a tracer. This interaction produces a bioluminescence resonance energy transfer (BRET) signal. The interaction between a second ligand and the target kinase competitively displaces the fluorescent tracer and reduces the BRET signal, thus showing that the competing ligand directly interacts with the target kinase in cells. These experiments used a construct expressing NanoLuc-PKN2$_{Ser646–Cys984}$ in cells and tracer 9 (Promega). Compounds **3**, **8**, **9** and **11** were assessed in dose–response measurements revealing IC_{50} values of 4.8, 2.1, 2.8 and 11 μM respectively (Fig. 4A). For **8** we made additional dose–response measurements at a range of tracer concentrations to both validate the quality of the data and estimate a value for the 'true' cellular IC_{50} in the absence of tracer, yielding a value of $IC_{50} = 1.1$ μM ± 0.45 (best fit value ± standard error) (Fig. 4B).

We next investigated the cellular toxicity of compounds **3**, **8**, and **9** using a cell viability assay based on the cellular metabolic conversion of soluble tetrazolium bromide (MTT) into insoluble formazan crystals in human (HeLa) cells. Our results indicated that cell viability was not severely affected by the compounds. At the highest concentration of 50 μM, the cells remained ≥70% viable 24 h after treatment. By contrast, treating these cells with the control staurosporine, a common promiscuous kinase inhibitor, had a profound impact on cell viability (Fig. 5). These results suggested that these dihydropyrrolopyridinone derivatives are not overtly toxic to human cells.

Previously, we optimized benzimidazole-based inhibitors to target PKN2 with 26-fold selectivity over PKN1. However, the most selective compound exhibited IC_{50} = 170 nM. The compounds in this series demonstrated improved potency towards PKN2, allowing for selectivity to be further developed and optimized at a later stage.

An existing crystal structure within the PDB (4F9B) suggests that the 4′-pyridyl of compound **3** is orientated towards a tyrosine residue (Tyr136) within the hinge region of cyclin-dependent kinase 7 (CDK7). It also shows the lactam oxygen interacting with a neighboring lysine residue (Lys90). This binding conformation agrees with the experimental data for **3** against PKN2 that shows the largest loss of potency across the series was when the 4′-pyridyl motif was altered, suggesting this interaction is key for binding. CDK7 is one of the targets shown to bind to compound **3** in the DiscoverX screen.

It is possible that the relatively small size of the A740 residue means that the nitrogen within the pyridine ring can form a hydrogen bond instead of relying on branching groups to accommodate optimal bond

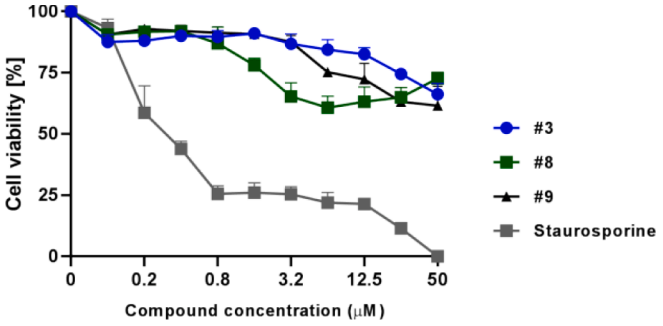

Fig. 5. Cell viability assay. Compound **3** and derivatives are not toxic to cells, with 70% of cells viable at the highest compound concentration tested (50 μM). The graphic represents a single experiment performed in triplicate (n = 1) with two independent biological replicates.

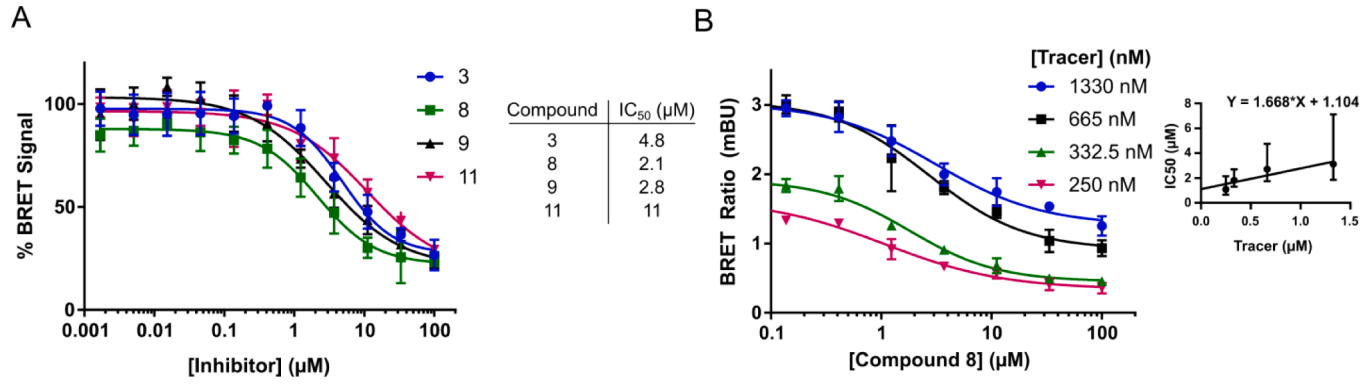

Fig. 4. Evaluation of compounds **3**, **8**, **9** and **11** binding to PKN2 in living cells. Nanoluc-PKN2$_{Ser646–Cys984}$ was overexpressed in HEK293 cells. **A.** Serially diluted inhibitors were assessed for their ability to displace a fluorescent tracer compound from PKN2. Compounds **3**, **8**, **9** and **11** had IC_{50} values against PKN2 of 4.8 ± 0.9 μM, 2.1 ± 0.4 μM, 2.8 ± 0.6 μM and 11 ± 4.8 μM respectively (mean ± SEM, n = 2 biological repeats). **B.** Compound **8** has a cellular IC_{50} for binding PKN2 of 1.1 μM in the absence of tracer as assessed by dose-responses of **8** at different tracer concentrations followed by linear regression of the IC_{50} values against tracer concentration.

angles within the hinge region of PKN2. Conversely, the larger L664 may limit proximity between bulky hydrogen bond donors/acceptors within the compounds and proteins, which may be why larger protruding groups from the 1-position resulted in loss of activity.

PKN2 is a protein kinase of interest in disease but currently lacks selective inhibitor compounds. We have demonstrated that a 20-fold selectivity can be achieved in vitro between PKN2 and close homologue, PKN1, exemplified by **3**. Optimization of this compound yielded PKN2-equipotent compounds **8** and **9** but did not improve on the initial PKN2/PKN1 selectivity.

Fewer than 5% of the 468 kinases available in the DiscoverX KINOME*scan*® panel were affected by compounds **3** and **8** at 1 μM concentration. Compounds **3**, **8** and **9** were also shown to be cell penetrant and showed little effect on cell viability in HeLa cells, indicating that they could be further optimized for use as chemical probes for studying PKN2.

Declaration of Competing Interest

The authors declare that they have no known competing financial interests or personal relationships that could have appeared to influence the work reported in this paper.

Acknowledgements

We thank MSc. Italo E.P. da Silva for the technical support in the platform of protein production. We thank Dr. Stanley N.S. Vasconcelos for the in silico analysis.

We also would like to thank the staff of the Life Sciences Core Facility (LaCTAD) from the State University of Campinas (UNICAMP) for mass spectrometry analysis. AMF and JET received CAPES fellowships (88887.136437/2017-00 and 88887.373547/2019-00). We declare there are no competing interests with any involved parties.

This work was supported by a Continuing Excellence Fund from the Genome Damage and Stability Centre, University of Sussex. Thanks also to additional funding from the Wellcome Trust for initial assay experiments. This work was also supported by the Brazilian agencies FAPESP (Fundação de Amparo à Pesquisa do Estado de São Paulo) (2014/50897-0) and CNPq (Conselho Nacional de Desenvolvimento Científico e Tecnológico) (465651/2014-3). The Structural Genomics Consortium is a registered charity (no: 1097737) that receives funds from Bayer AG, Boehringer Ingelheim, Bristol Myers Squibb, Genentech, Genome Canada through Ontario Genomics Institute [OGI-196], EU/EFPIA/OICR/McGill/KTH/Diamond Innovative Medicines Initiative 2 Joint Undertaking [EUbOPEN grant 875510], Janssen, Merck KGaA (aka EMD in Canada and US), Pfizer and Takeda.

Appendix A. Supplementary data

Supplementary data to this article can be found online at https://doi.org/10.1016/j.bmcl.2022.128588.

References

1 Mukai H. The structure and function of PKN, a protein kinase having a catalytic domain homologous to that of PKC. *J Biochem*. 2003;133(1):17–27. https://doi.org/10.1093/jb/mvg019.
2 Palmer RH, Ridden J, Parker PJ. Identification of multiple, novel, protein kinase C-related gene products. *FEBS Lett*. 1994;356(1):5-8. doi:0014-5793(94)01202-4 [pii].
3 Kitagawa M, Mukai H, Shibata H, Ono Y. Purification and characterization of a fatty acid-activated protein kinase (PKN) from rat testis. *Biochem J*. 1995;310(2):657–664. https://doi.org/10.1042/bj3100657.
4 Mukai H, Kitagawa M, Shibata H, et al. Activation of PKN, a novel 120-kDa protein kinase with leucine zipper-like sequences, by unsaturated fatty acids and by limited proteolysis. *Biochem Biophys Res Commun*. 1994;204(1):348–356. https://doi.org/10.1006/bbrc.1994.2466.
5 Hashimoto T, Mukai H, Kawamata T, Taniguchi T, Ono Y, Tanaka C. Localization of PKN mRNA in the rat brain. *Mol Brain Res*. 1998;59(2):143–153. https://doi.org/10.1016/S0169-328X(98)00155-7.
6 Quilliam LA, Lambert QT, Mickelson-Young LA, et al. Isolation of a NCK-associated kinase, PRK2, an SH3-binding protein and potential effector of Rho protein signaling. *J Biol Chem*. 1996;271(46):28772–28776. https://doi.org/10.1074/jbc.271.46.28772.
7 Palmer RH, Dekker LV, Woscholski R, Le Good JA, Gigg R, Parker PJ. Activation of PRK1 by phosphatidylinositol 4,5-bisphosphate and phosphatidylinositol 3,4,5-trisphosphate: A comparison with protein kinase C isotypes. *J Biol Chem*. 1995;270(38):22412–22416. https://doi.org/10.1074/jbc.270.38.22412.
8 Van Aelst L, D'Souza-Schorey C. Rho GTPases and signaling networks. *Genes Dev*. 1997;11(18):2295–2322. https://doi.org/10.1101/gad.11.18.2295.
9 Schmidt A, Durgan J, Magalhaes A, Hall A. Rho GTPases regulate PRK2/PKN2 to control entry into mitosis and exit from cytokinesis. *EMBO J*. 2007;26(6):1624–1636. https://doi.org/10.1038/sj.emboj.7601637.
10 Gampel A, Parker PJ, Mellor H. Regulation of epidermal growth factor receptor traffic by the small GTPase RhoB. *Curr Biol*. 1999;9(17):955–958. https://doi.org/10.1016/S0960-9822(99)80422-9.
11 Takagi H, Hsu C-P, Kajimoto K, et al. Activation of PKN mediates survival of cardiac myocytes in the heart during ischemia/reperfusion. *Circ Res*. 2010;107(5):642–649. https://doi.org/10.1161/CIRCRESAHA.110.217554.
12 Lachmann S, Jevons A, De Rycker M, et al. Regulatory domain selectivity in the cell-type specific PKN-dependence of cell migration. *PLoS ONE*. 2011;6(7):e21732. https://doi.org/10.1371/journal.pone.0021732.
13 Behan FM, Iorio F, Picco G, et al. Prioritization of cancer therapeutic targets using CRISPR–Cas9 screens. *Nature*. 2019;568(7753):511–516. https://doi.org/10.1038/s41586-019-1103-9.
14 Lin W, Huang J, Yuan Z, Feng S, Xie Y, Ma W. Protein kinase C inhibitor chelerythrine selectively inhibits proliferation of triple-negative breast cancer cells. *Sci Rep*. 2017;7(1):2022. https://doi.org/10.1038/s41598-017-02222-0.
15 Yang C-S, Melhuish TA, Spencer A, et al. The protein kinase C super-family member PKN is regulated by mTOR and influences differentiation during prostate cancer progression. *Prostate*. 2017;77(15):1452–1467. https://doi.org/10.1002/pros.23400.
16 Aleku M, Schulz P, Keil O, et al. Atu027, a liposomal small interfering RNA formulation targeting protein kinase N3, inhibits cancer progression. *Cancer Res*. 2008;68(23):9788–9798. https://doi.org/10.1158/0008-5472.CAN-08-2428.
17 Santel A, Aleku M, Röder N, et al. Atu027 prevents pulmonary metastasis in experimental and spontaneous mouse metastasis models. *Clin Cancer Res*. 2010;16(22):5469–5480. https://doi.org/10.1158/1078-0432.CCR-10-1994.
18 Structural Genomics Consortium. Chemical Probes. Accessed September 12, 2021. https://www.thesgc.org/chemical-probes.
19 Mendez D, Gaulton A, Bento AP, et al. ChEMBL: Towards direct deposition of bioassay data. *Nucleic Acids Res*. 2019;47(D1):D930-D940. doi:10.1093/nar/gky1075.
20 Scott F, Fala AM, Pennicott LE, et al. Development of 2-(4-pyridyl)-benzimidazoles as PKN2 chemical tools to probe cancer. *Bioorg Med Chem Lett*. 2020;30(8):127040. https://doi.org/10.1016/j.bmcl.2020.127040.
21 Anderson DR, Meyers MJ, Vernier WF, et al. Pyrrolopyridine inhibitors of mitogen-activated protein kinase-activated protein kinase 2 (MK-2). *J Med Chem*. 2007;50(11):2647–2654. https://doi.org/10.1021/jm061100410.1021/jm0611004.s001.
22 Roskoski R. Properties of FDA-approved small molecule protein kinase inhibitors: a 2020 update. *Pharmacol Res*. 2020;152:104609. https://doi.org/10.1016/j.phrs.2019.104609.
23 Surase YB, Samby K, Amale SR, et al. Identification and synthesis of novel inhibitors of mycobacterium ATP synthase. *Bioorg Med Chem Lett*. 2017;27(15):3454–3459. https://doi.org/10.1016/j.bmcl.2017.05.081.
24 Yung-Chi C, Prusoff WH. Relationship between the inhibition constant (KI) and the concentration of inhibitor which causes 50 per cent inhibition (I50) of an enzymatic reaction. *Biochem Pharmacol*. 1973;22(23):3099–3108. https://doi.org/10.1016/0006-2952(73)90196-2.
25 Meredith EL, Ardayfio O, Beattie K, et al. Identification of orally available naphthyridine protein kinase D inhibitors. *J Med Chem*. 2010;53(15):5400–5421. https://doi.org/10.1021/jm100075z.
26 Posy SL, Hermsmeier MA, Vaccaro W, et al. Trends in kinase selectivity: insights for target class-focused library screening. *J Med Chem*. 2011;54(1):54–66. https://doi.org/10.1021/jm101195a.
27 Robers MB, Dart ML, Woodroofe CC, et al. Target engagement and drug residence time can be observed in living cells with BRET. *Nat Commun*. 2015;6(1). https://doi.org/10.1038/ncomms10091.